Monitoring helicase activity with molecular beacons

Craig A. Belon and David N. Frick

BioTechniques 45:433-442 (October 2008)
doi 10.2144/000112834

A high-throughput, fluorescence-based helicase assay using molecular beacons is described. The assay is tested using the NS3 helicase encoded by the hepatitis C virus (HCV) and is shown to accurately monitor helicase action on both DNA and RNA. In the assay, a ssDNA oligonucleotide molecular beacon, featuring a fluorescent moiety attached to one end and a quencher attached to the other, is annealed to a second longer DNA or RNA oligonucleotide. Upon strand separation by a helicase and ATP, the beacon strand forms an intramolecular hairpin that brings the tethered fluorescent and quencher molecules into juxtaposition, quenching fluorescence. Unlike currently available real-time helicase assays, the molecular beacon–based helicase assay is irreversible. As such, it does not require the addition of extra DNA strands to prevent products from re-annealing. Several variants of the new assay are described and experimentally verified using both Cy3 and Cy5 beacons, including one based on a sequence from the HCV genome. The HCV genome–based molecular beacon helicase assay is used to demonstrate how such an assay can be used in high-throughput screens and to analyze HCV helicase inhibitors.

INTRODUCTION

Helicases are motor proteins that unwind double-stranded nucleic acids by utilizing free energy from ATP hydrolysis. They are ubiquitous enzymes in the cellular milieu, functioning in diverse processes including DNA replication, DNA repair, RNA transcription, and translation (1). The genomes of all cellular pathogens and many viruses code for helicases, and there has been great interest in exploiting helicases as potential drug targets. However, with the exception of several potent compounds that inhibit a helicase encoded by herpes simplex virus, few helicase inhibitors have entered clinical trials (2). One explanation for slow helicase inhibitor development may be that helicase activity is complex to monitor, making inhibitor identification and analysis difficult. Therefore, the goal of this study is to develop an improved helicase assay that could be used both for high-throughput screening and mechanistic analyses. Here, we describe how molecular beacons commonly used for quantitative PCR can serve this purpose.

Typically, helicase activity is measured by incubating a helicase with ATP and a radiolabeled DNA duplex, terminating the reaction, and analyzing the products using non-denaturing PAGE (3). Although such assays can be used to extract reaction details, they are cumbersome, time-consuming, and only yield a single time point for each reaction performed. This basic helicase assay can be performed in a high-throughput format by filtering the products after the reaction is stopped (4), or by using radiolabeled biotinylated oligonucleotides in a scintillation proximity assay (5). Electrochemiluminescence used with ruthenium-labeled biotinylated oligonucleotides (6) can circumvent the need for the radioactive biohazard. Nevertheless, all such assays only yield a single time point per reaction, limiting their potential usefulness.

Fluorescence has been the main tool used to date to increase the number of time points recorded in a single helicase reaction. To this end, fluorescent nucleotides can be incorporated into DNA (7), two fluorescent moieties tethered to opposing strands (8–10), or fluorescent intercalating agents added to DNA (11). Each of these assays can be used to monitor DNA (or RNA) unwinding in real time, but each has its own set of drawbacks. For example, most fluorescent nucleotide analogs [with the exception of 2-aminopurine (7)] disrupt Watson-Crick base pairing, fluorescent moieties or DNA ligands could affect unwinding rates, and ssDNA traps need to be added to such assays to prevent the substrate from re-annealing.

To better monitor helicase action, we have designed a fluorescence-based assay using molecular beacons: single-stranded nucleic acid molecules that form stem loop structures. One end of the molecular beacon is attached to a fluorescent molecule and the other to a quencher such that, upon strand separation and subsequent formation of the stem-loop structure, fluorescence is quenched (12). Intramolecular hairpin formation prevents strand re-annealing, and eliminates the need for the addition of ssDNA trap molecules to the reaction mixture. Furthermore, since most helicases typically contact one strand of a duplex more than its complement (13,14), the design of these new helicase substrates helps minimize the possible impact of the modifications on observed reaction rates.

As a model helicase to test this assay, we used a recombinant enzyme derived from hepatitis C virus (HCV) (15). HCV causes a liver disease that affects more than two percent of the world population. The virus itself is a positive-sense ssRNA virus coding for a single polyprotein that is cleaved into structural and non-structural proteins. One of the non-structural proteins is a multifunctional enzyme possessing an N-terminal protease domain and a

Department of Biochemistry and Molecular Biology, New York Medical College, Valhalla, NY, USA

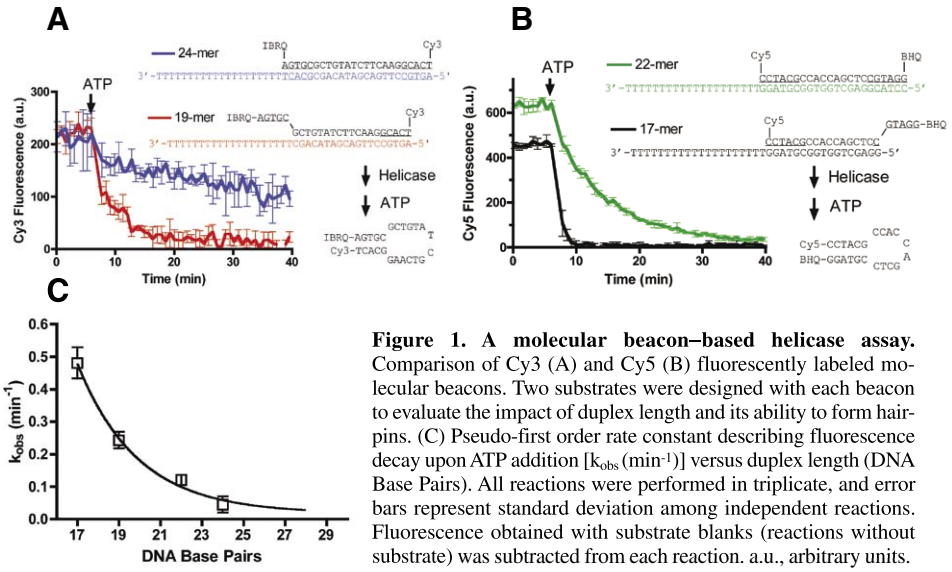

Figure 1. A molecular beacon–based helicase assay. Comparison of Cy3 (A) and Cy5 (B) fluorescently labeled molecular beacons. Two substrates were designed with each beacon to evaluate the impact of duplex length and its ability to form hairpins. (C) Pseudo-first order rate constant describing fluorescence decay upon ATP addition [k_{obs} (min^{-1})] versus duplex length (DNA Base Pairs). All reactions were performed in triplicate, and error bars represent standard deviation among independent reactions. Fluorescence obtained with substrate blanks (reactions without substrate) was subtracted from each reaction. a.u., arbitrary units.

Table 1. Sequences of Oligonucleotides Used

Description	Figure	Sequence
Cy3 top strand	1A, 2A, 3A	5′-/IBRQ/AGTGCGCTGTATCGTCAAGGCACT/Cy3/-3′
Cy5 top strand	1B, 3A	5′-/Cy5/CCTACGCCACCAGCTCCGTAGG/BHQ/-3′
Cy3 bottom strand	1A, 2A	5′-AGTGCCTTGACGATACAGC$(T)_{20}$-3′
Cy3 bottom strand (RNA)	2A	5′-AGUGCCUUGACGAUACAGC$(U)_{20}$-3′
Cy5 bottom strand	1B	5′-GGAGCTGGTGGCGTAGG$(T)_{20}$-3′
Hairpin Cy3 bottom strand	1A	5′-AGTGCCTTGACGATACAGCGCACT$(T)_{19}$-3′
Hairpin Cy5 bottom strand	1B	5′-CCTACGGAGCTGGTGGCGTAGG$(T)_{20}$-3′
FRET bottom strand	3A	5′-GGAGCTGGTGGCGTAGGCAAGAGTGCCTTGACGA TACAGC$(T)_{20}$-3′
HCV genome top strand	4A	5′-/Cy5/GCTCCCCAATCGATGAACGGGGAGC/IBQ/-3′
HCV genome bottom strand	4A	5′-GCTCCCCGTTCATCGATTGGGGAGC$(T)_{20}$

Underlined regions correspond to hairpin-forming residues.

C-terminal ATPase/helicase domain. The helicase portion of non-structural protein 3 (NS3) is needed for HCV RNA replication (16,17), but while many potent small molecule inhibitors for this helicase target have been discovered (18–21), none have entered the clinic. Many assays specific for HCV helicase activity have been developed—such as those based on ELISA (22), scintillation proximity assays (23), flashplate methods (24), and FRET (25,26)—but they all suffer from the same drawbacks as the aforementioned general helicase assays.

Here we develop a simple assay for evaluating helicase activity based on molecular beacon technology and demonstrate its usefulness using HCV helicase as a model. Our new assay is advantageous because it is continuous, does not require modification of the strand on which the helicase translocates, is essentially irreversible, and eliminates the need for the addition of extra DNA to capture displaced strands. The assay should be useful for mechanistic analyses, is amenable to high-throughput screening, and could be used to rapidly evaluate enzyme inhibitors.

MATERIALS AND METHODS

Materials

DNA and RNA oligonucleotides were purchased from Integrated DNA Technologies (Coralville, IA, USA) in purified form as lyophilized solids. They were then dissolved in DNase/RNase-free water (FisherBiotech, Fair Lawn, NJ, USA), and concentrations were determined from the extinction coefficients provided. Oligonucleotides were modified with Cyanine 3 (Cy3), Cyanine 5 (Cy5), Iowa Black RQ (IBRQ), and Black Hole Quencher (BHQ) (Integrated DNA Technologies). The sequences of the oligonucleotides used in the study are noted in Table 1.

Helicase substrates were prepared by combining single strands at a 1:1 molar ratio to a final concentration of 20 µM in 10 mM Tris-HCl pH 8.5, placing in 95°C water, and allowing to cool to room temperature for ~1 h to anneal.

The HCV NS3 helicase enzyme used for this study was a recombinant protein derived from the HCV 1b genotype, lacking the N-terminal NS3 protease domain. Cloning, expression, and purification of this truncated NS3 protein has been described before (27). It contains a C-terminal His-tag consisting of the sequence "PNSSS VDKLA AALEH HHHHH." Protein concentrations were determined by absorbance at 280 nm using extinction coefficients calculated using the Sequence Analysis program (http://informagen.com/SA).

Molecular beacon–based unwinding assay

Unless otherwise noted, each reaction contained 25 mM MOPS pH 6.5, 2 mM $MgCl_2$, 25 nM enzyme, 5 nM nucleic acid substrate, and was initiated with 0.5 mM ATP. Reactions were carried out in 100 µL, in triplicate, in white half-volume 96-well polystyrene plates at 22°C. Fluorescence was measured as arbitrary units (a.u.) in each well every 40 s when using a 96-well plate. Data were collected using a Cary eclipse fluorescence spectrophotometer equipped with the microplate reader accessory (Varian, Inc., Palo Alto, CA, USA). Cy3-labeled substrates were measured for excitation/emission at 552/570 nm (5/10 nm slit width). Cy5-labeled substrates were similarly measured at 643/667 nm and FRET measured at 570/667 nm. Stopped-flow data was collected using an RX.2000 rapid kinetics spectrophotometer accessory (Applied Photophysics, Leatherhead, UK) with 1.0 mM ATP in syringe A and 2× reaction mixture in syringe B (50 mM MOPS pH 6.5, 4 mM $MgCl_2$, 50 nM enzyme, 10 nM nucleic acid substrate). Reactions were started by mixing syringe A and B in a 1:1 ratio such that final concentrations of all components were identical to those for the plate-based assays.

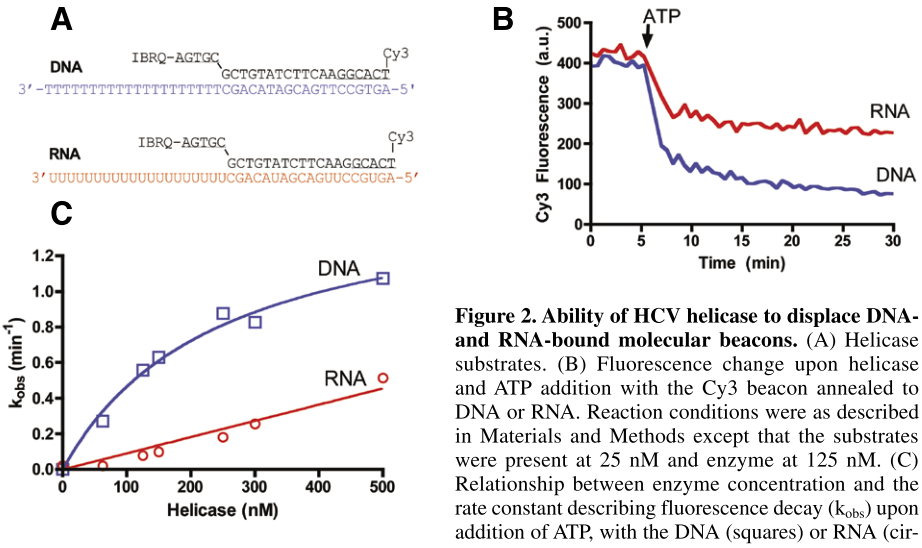

Figure 2. Ability of HCV helicase to displace DNA- and RNA-bound molecular beacons. (A) Helicase substrates. (B) Fluorescence change upon helicase and ATP addition with the Cy3 beacon annealed to DNA or RNA. Reaction conditions were as described in Materials and Methods except that the substrates were present at 25 nM and enzyme at 125 nM. (C) Relationship between enzyme concentration and the rate constant describing fluorescence decay (k_{obs}) upon addition of ATP, with the DNA (squares) or RNA (circles) substrate. a.u., arbitrary units.

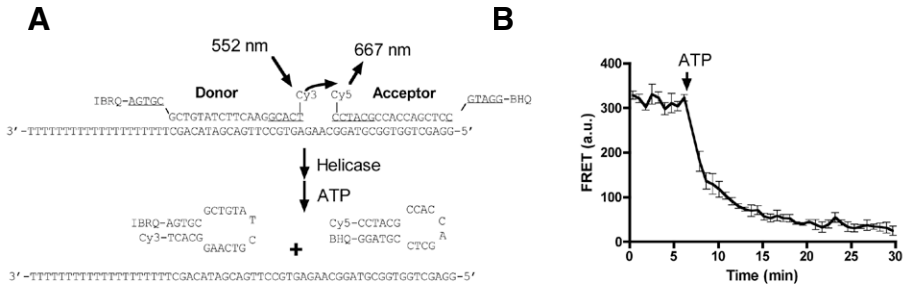

Figure 3. FRET-based assay using molecular beacons. (A) Substrate. The signal caused by loss of FRET corresponds to the separation of the donor strand, a region of 19 bp. (B) Change in FRET in a helicase substrate complex following ATP addition. The first order rate constant describing fluorescence decay, k_{obs}, is 0.23 for this reaction, very similar to that seen with the 19 bp substrate from Figure 1A. Fluorescence obtained with substrate blanks (reactions without substrate) is subtracted from each reaction. Error bars represent standard deviation of triplicate reactions.

Data were analyzed using Graphpad Prism 4.0 (San Diego, CA, USA), and a first-order exponential decay model was used to determine the pseudo-first order rate constant, k_{obs}. Data are shown with error bars of 1 standard deviation.

Radioactive unwinding assay

5′-^{32}P–labeled HCV genome template DNA was prepared by incubating 2 µL of 10 µM oligonucleotide, 4 µL of [γ^{32}P]ATP (0.5 mCi, MP Biomedical, Solon, OH, USA), 2 µL 10× reaction buffer (New England Biolabs, Ipswich, MA, USA), 1 µL polynucleotide kinase (New England Biolabs) and 11 µL of water for 1 h at 37°C. The resulting labeled oligonucleotide was purified using a QIAquick Nucleotide Removal Kit (Qiagen, Valencia, CA, USA). Concentration was determined by measuring A_{260} with ε = 389400 $M^{-1}cm^{-1}$. The helicase substrate was then made as noted above.

Reaction conditions were identical to those used for continuous fluorescent assays. All reactants except ATP were added to the well, and 10 µL placed into 2.5 µL of stopping buffer for a t_0 point. The ATP was added, and 10 µL aliquots removed and placed into 2.5 L of 5× stopping buffer after 20 s, 40 s, 1 min, 2 min, 3 min, 5 min, 7.5 min, 10 min, and 20 min. 5× stopping buffer contained 250 mM TRIS-Cl pH 7.5, 20 mM EDTA, 0.5% SDS, 0.1% Nonidet P-40, 0.1% bromophenol blue, 0.1% xylene cyanol FF, and 50% glycerol. Four microliters of each quenched aliquots (4 nM DNA) were run on a 12% non-denaturing polyacrylamide gel at a constant 200 V for 30 min. Radiolabeled ssDNA (2 µL of 37.5 nM ssDNA in stopping buffer) and substrate DNA (2 µL of 25 nM DNA in stopping buffer) controls were

included. The gels were dried, exposed to a PhosphorImager screen for 14 h and imaged using a Storm 860 scanner (Molecular Dynamics, Sunnyvale, CA, USA), and quantified with ImageJ software (http://rsb.info.nih.gov/ij). Substrate fraction was calculated and corrected for the presence of ssDNA at t_0 using Equation 1:

$$\text{Substrate fraction} = \frac{DS(DS_0 + SS_0)}{DS_0(DS + SS)}, \quad \text{[Eq.1]}$$

where *DS* and *SS* are radioactive intensities for dsDNA and ssDNA at a given time and DS_0 and SS_0 are radioactive intensities at t_0, respectively.

High-throughput screening

Two separate reactions, a positive control (no inhibitor) and negative control (dT_{20}), were used. In both instances, the HCV-derived DNA substrate shown in Figure 4A was used. These reactions were staggered in a checkerboard pattern on a 384-well plate. The no-inhibitor reactions were identical to those described above for the real-time assay. For a negative control dT_{20} inhibited reaction, the mixture contained an additional 1 µM of dT_{20}, a short ssDNA that competes with the dsDNA substrate. For each well, only two data points were collected: one before the addition of ATP (F_0) and one at 30 min (F_{30}). F_0 was simply used as a quality control to ensure that the inhibitor did not itself cause quenching of fluorescence; only F_{30} was evaluated to determine reaction progress. Z′ factors (28) were determined with Equation 2:

$$Z' = 1 - \frac{3(\sigma_p + \sigma_n)}{|\mu_p - \mu_n|}, \quad \text{[Eq. 2]}$$

where σ_p and σ_n are the standard deviations of the positive and negative controls, respectively, and μ_p and μ_n are similarly the means of the positive and negative controls. Pilot uninhibited and inhibited reactions (n = 16) were monitored continuously for fluorescence. Experiments with n = 103 or 104 only used the F_{30} data point to compute quantitative parameters. The coefficient of variance (CV) was determined as shown in Equation 3:

$$CV = \frac{\sigma}{\mu} \times 100, \quad \text{[Eq. 3]}$$

where σ is the standard deviation and µ is average of all points read at 30 min.

To determine repeatability and day-to-day variability of the assay, inhibited and uninhibited controls in

384-well white plates were conducted on different days using the Eclipse Fluorescence Spectrophotometer (Varian, Inc.). To optimize assay sensitivity, the same reactions were performed in 384-well black plates and read with a Tecan Infinite M200 Fluorescence Microplate Reader (Männendorf, Switzerland).

RESULTS

Molecular beacons, hairpin oligonucleotides modified at either end with a fluorophore and quencher, are commonly used to measure DNA concentrations during real-time polymerase chain reactions. In real-time PCR, an increase in fluorescence is observed when the molecular beacon anneals to amplified DNA. We hypothesized that if a corresponding reciprocal decrease in fluorescence occurs when the beacon is separated from its target DNA, then such a signal could be used to monitor the action of a DNA or RNA helicase. To test this idea, we used an enzyme capable of unwinding duplex DNA or RNA, the HCV NS3 protein, and molecular beacons previously shown to anneal to either DNA or RNA (29). Although most helicases prefer to unwind either DNA or RNA, HCV helicase has a uniquely relaxed specificity; even though HCV is an RNA virus and the helicase likely never encounters DNA, the recombinant protein actually unwinds DNA better than RNA (30).

Cy3- and Cy5-based molecular beacons in helicase assays

To examine the consequence of HCV helicase displacing DNA-bound molecular beacons, four different duplexes were generated with either Cy3- (Figure 1A) or Cy5- (Figure 1B) labeled probes. Each probe was annealed either to an oligonucleotide that could form an intermolecular hairpin (longer duplex) or one that could not (shorter duplex). HCV NS3 helicase must first bind to a ssDNA region as it moves from 3′ to 5′ unwinding a duplex, so long strands were designed with a 20 nucleotide long 3′ overhang consisting of 20 dT residues for DNA templates, or a 3′-U_{20} overhang for the RNA template strand.

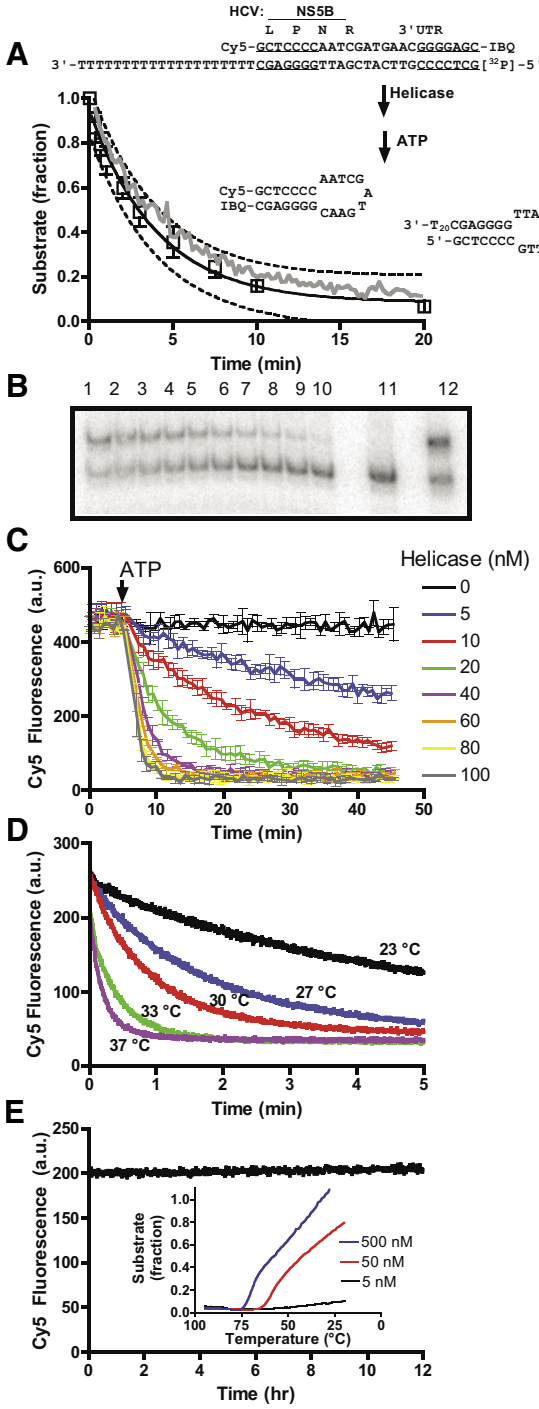

Figure 4. A HCV genome–based molecular beacon assay. (A) Comparison of a molecular beacon–based assay to a conventional electrophoretic mobility shift (EMSA) gel-based helicase assay. Two simultaneous reactions were run with the substrate shown. One was monitored continuously for fluorescence (gray line), and aliquots were removed from the other and analyzed on three separate gels (squares). Fluorescence obtained from substrate blanks is subtracted and fractional fluorescence (F/F_o) is plotted. The error bars denote the standard deviation among the EMSAs and the dashed line represents the 95% confidence band for data derived from the EMSAs. (B) Sample gel from one of the EMSAs. Lane 1 represents an aliquot removed before adding ATP to start the reaction (t_0); lanes 2–10 represent aliquots removed after 20 s, 40 s, 1 min, 2 min, 3 min, 5 min, 7.5 min, 10 min, and 20 min. Lane 11 is the [^{32}P] oligonucleotide alone and lane 12 is substrate alone. (C) The unwinding reaction as a function of helicase concentration. Error bars represent standard deviation of triplicate reactions. (D) The unwinding reaction (25 nM helicase) as a function of temperature. Because of the rapid progress of the reaction at elevated temperatures, these data were collected using a rapid-mixing stopped-flow device. (E) Substrate stability. Very little fluorescence change is observed for 12 h when the substrate is incubated in reaction buffer without enzyme or ATP at 22°C (black line). The inset shows annealing curves for the same substrate at 5 nM (black), 50 nM (red), and 500 nM (blue). Fluorescence was monitored while decreasing temperature from 95°C. a.u., arbitrary units.

In reactions incubated with the DNA substrate and HCV helicase alone, the fluorescence did not change. However, when ATP was added to the reaction, a rapid decrease in fluorescence was observed. Reactions were reproducible, with triplicate independent reactions yielding fluorescence traces that overlaid almost perfectly.

Hairpin formation by either strand of the substrate did not prevent the helicase from unwinding the duplex. Fluorescence decay fit well to a first order equation and the observed rate constants describing the reaction are proportional to the duplex length (Figure 1C). Results were similar with both Cy3 and Cy5 beacons. However, the same amount of Cy5 probes produced stronger signals than Cy3-based beacons, with lower signal-to-noise ratios (Figure 1, A and B). It is important to note that most reactions proceeded to completion in

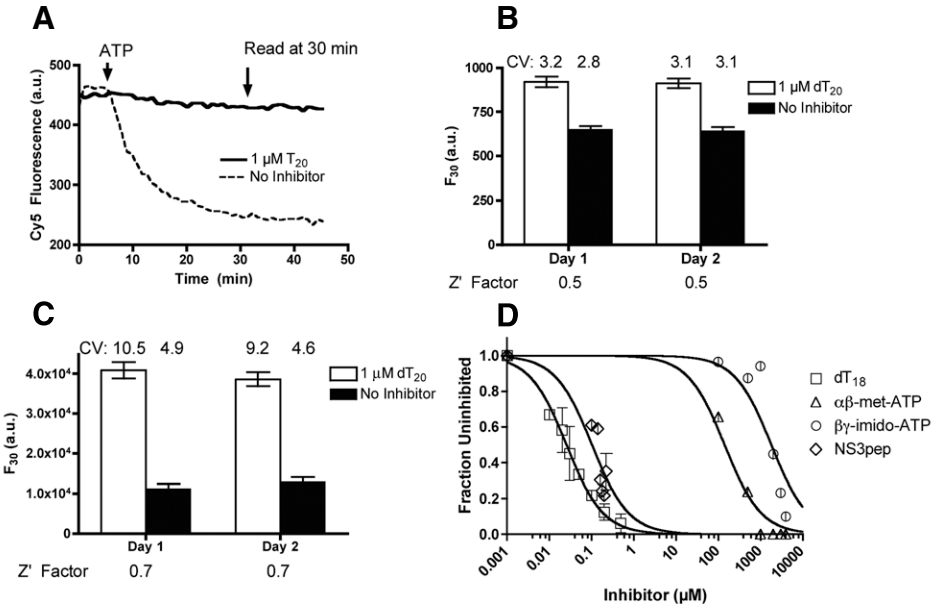

Figure 5. High-throughput screening. (A) Representative data from two continuously monitored inhibited and non-inhibited reactions. (B and C) 104 inhibited and 103 non-inhibited reactions, carried out simultaneously in a 384-well plate with a final reaction volume of 50 µL. Identical sets of the same reactions were repeated on two different days. (B) Data obtained with a Cary Eclipse microplate reader with excitation/emission measured at 643/667 nm (slit widths of 5/10 nm, respectively) (C) Data obtained with black plates in a Tecan microplate reader with excitation/emission measured at 643/670 nm (9/20 nm slit widths). Substrate blanks (reactions without substrates) were not subtracted from reactions. (D) Data using the fluorescent assay to evaluate four inhibitors. dT_{18} competes with the DNA substrate, while α,β-methylene-ATP and β,γ-imido-ATP are non-hydrolyzable ATP analogs that compete with ATP. NS3pep is a potent, newly described peptide inhibitor of NS3 helicase with the sequence RRGRTGRGRRGIYR (33). a.u., arbitrary units. Error bars represent standard deviation of triplicate reactions.

the timescale measured, even in the absence of trap DNA used to capture the dissociated DNA. This result stands in stark contrast to other fluorescent HCV helicase assays, which absolutely require the presence of a capture strand (25,26).

With the 17-mer substrate shown in Figure 1B, it is conceivable that the helicase could simultaneously load and unwind along the 3′-ssDNA regions of both strands. To test this, the Cy5 beacon was annealed to an oligonucleotide lacking the 3′-dT_{20} leader sequence. When this blunt-end substrate was used in the same helicase assay, no change in fluorescence occurred, indicating the enzyme was not unwinding from the 3′-BHQ-GGATG end (data not shown).

The same beacons were then used to analyze the action of HCV helicase on RNA (Figure 2A). With RNA, the beacons fluoresced strongly only when annealed to complementary strands that do not form intermolecular hairpins (i.e., those that form the 17- and 19-mer duplexes). This may be due to the fact that RNA secondary structures are more stable than comparable DNA structures or that duplex RNA structures are less stable than a DNA double helix. Regardless, the shorter RNA-DNA heteroduplexes fluoresced at levels similar to that seen with the DNA duplex (Figure 2B). When incubated with HCV helicase and ATP, the fluorescence of the RNA-DNA duplex likewise rapidly decreased. Both the initial rates and final amplitude of the fluorescence decrease were lower when the beacons were annealed to RNA (Figure 2B). With both DNA and RNA, observed rate constants (and thus initial reaction rates) were linear with enzyme concentration. However at each enzyme concentration, RNA was unwound more slowly than DNA (Figure 2C), as is typically seen with this enzyme (15).

Dual FRET molecular beacons can be used to determine DNA unwinding

To further evaluate molecular beacon–based helicase assays using another technique, we combined the two molecular beacon substrates shown in Figure 1 to produce a dual FRET molecular beacon, based on one developed by Santangelo et al. (29) (Figure 3A). In this setup, two beacons were annealed to the same oligonucleotide such that Cy3 emitted light that could be absorbed by Cy5. The displacement of either probe would therefore lead to a subsequent decrease in FRET between Cy3 and Cy5. To test this, the dual FRET molecular beacon was used under our standard helicase assay conditions, and FRET decreased only after addition of the helicase and ATP (Figure 3B). Again, the signal was highly reproducible and rates of decrease were proportional to the amount of enzyme in solution.

An HCV genome–based molecular beacon helicase assay

Since our goal is to eventually use this assay to screen for HCV inhibitors, we also designed another helicase substrate based on a hairpin-forming region of the HCV genome located at the end of the open reading frame encoding the HCV polyprotein near the 3′ untranslated region (Figure 4A). Using the HCV substrate, we performed simultaneous experiments with the beacon annealed to a radiolabeled oligonucleotide. We measured fluorescence continuously in one well and used a conventional gel-based electrophoretic mobility shift assay (EMSA) to analyze fractions removed from another well (Figure 4B).

Upon incubation with HCV helicase and ATP, a fluorescence decrease was again observed and when raw fluorescence was converted to fractional fluorescence remaining, the data were overlaid with that obtained from a standard assay (Figure 4A). When each data set is fit to a first-order rate equation, the k_{obs} obtained with fluorescence (0.22 min^{-1}) was slightly slower than that obtained with an EMSA (0.25 min^{-1}). To examine if this difference was due to a slower change in fluorescence (possibly due to hairpin formation, for example) or experimental error, the same samples were analyzed on two additional gels (error bars, Figure 4A). The dotted lines on Figure 4A show the 95% prediction band for the best-fit curve of the three EMSA data sets. The fluorescence data all fit within

this range, demonstrating that the slight differences in rates are likely due to error introduced during the elaborate EMSA. Helicase activity was also monitored at varying concentrations of enzyme (Figure 4C) in well plates, as well as at different temperatures using a stopped-flow device due to the shorter reaction times at elevated temperature (Figure 4D).

The gel in Figure 4B reveals that there was a considerable amount of ssDNA present before ATP addition (lane 1), which is equivalent to the amount of free ssDNA in the substrate after annealing (lane 12) where the material is about 65% dsDNA. Because the ssDNA in the starting material could be due either to substrate instability or incomplete annealing, we performed experiments to judge the stability and annealing of the molecular beacon substrates. The two Cy5-labeled substrates from Figure 1B and the one from Figure 4A (17, 22, and 25 bp, respectively) were monitored for fluorescence at 22°C in the absence of enzyme and ATP. No fluorescence decrease was observed after 12 h, indicating the substrates were very stable and did not spontaneously separate (Figure 4E). To examine substrate annealing, the constituent strands of each DNA substrate were combined and fluorescence monitored to judge annealing at 22°C. At 5 nM, the half-times of annealing for the 17- and 22-bp substrates were 1.5 and 4.6 h respectively, while the 25-bp substrate only annealed to 10% of its maximum fluorescence after 12 h (data not shown). Even upon heating to 95°C, the 25-bp substrate showed little annealing at 5 nM. The fraction annealed after heating to 95°C increased significantly at 50 and 500 nM (Figure 4E, inset). We conclude that incomplete annealing leads to the ssDNA contamination of the substrate (Figure 4B, lane 12).

The presence of ssDNA in helicase substrates is common and is dealt with by either using an accounting equation (e.g., Equation 3 of Reference 31) or by purifying the substrates with the use of native polyacrylamide gels (32). Here we used Equation 1 (see Radioactive unwinding assay section) to correct for ssDNA contaminates, but we also purified the substrates on gels (data not shown). The fluorescent labels used here permit direct DNA visualization without dyes or UV light, greatly facilitating purification. Thus, we recommend such purification if these substrates are used in mechanistic studies since helicases bind ssDNA and slower rates would be observed with contaminated substrates. Additionally, mechanistic studies would require a comparison of data obtained with fluorescent beacons to data obtained with the same DNA substrate lacking fluorescent moieties.

High-throughput screening

To determine if a molecular beacon–based helicase assay is suitable for high-throughput screening (HTS), a series of pilot screens were conducted using the HCV-based substrate (Figure 5). All reactions were the same as those described in Figure 4A except that they were performed in 384-well plates at a volume of 50 µL. 16 pilot reactions—8 uninhibited and 8 inhibited with an oligonucleotide decoy substrate (1 µM dT_{20})—were monitored continuously to follow reaction progress. After determining that the positive control reaction was near complete after 30 min (Figure 5A), the rest of the reactions were only read twice: before ATP addition and 30 min after ATP addition. Next, pilot screens were each carried out with 104 inhibited and 103 uninhibited control reactions per plate. Positive and negative control reactions were staggered in a checkerboard pattern on the 384-well plate. 30 min after the start of the reaction, fluorescence from inhibited and uninhibited reactions was statistically different (Figure 5B). To examine day-to-day repeatability of the assay, additional assays were performed under identical conditions on another day with nearly identical results. Although the assay-to-assay precision was high in a Cary Eclipse plate reader (Varian, Inc.) (CVs ~3%), we were somewhat disappointed by

the relative low Z′ factors (0.5). We reasoned that the low score might be due to low instrument sensitivity. The Varian instrument is not compatible with standard black microplates and as a result a relatively high background is seen from the necessary white plates. We therefore repeated the high-throughput screen in black 384-well plates using a Tecan microplate reader, again with two separate sets of reactions on 2 d. Although results with the Tecan instrument were somewhat less precise (CVs 5%–10%) the Z′ factor was significantly higher at 0.7, indicating an excellent high-throughput assay (Figure 5C).

To demonstrate how this assay can be used to characterize various classes of NS3 inhibitors, we compared various known inhibitors with the oligonucleotide dT_{18}, a representative compound that binds in place of the RNA or DNA substrate. Two non-hydrolyzable ATP analogs (α,β–methylene-ATP and β,γ–imido-ATP) that compete with ATP binding, and a newly reported peptide inhibitor, NS3pep (RRGRTGRGRRGIYR) (33), were analyzed. All reactions were performed in triplicate and IC_{50} values were calculated using a sigmoidal dose-response curve. The oligonucleotide dT_{18} was the most potent inhibitor with an IC_{50} of 30 nM, NS3pep inhibited with an IC_{50} of 100 nM, and the ATP analogs bound much more weakly: α,β–methylene-ATP had an IC_{50} of 140 μM, which was more than 10 times lower than β,γ–imido-ATP, with an IC_{50} of 1.8 mM (Figure 5D).

DISCUSSION

Here we describe a new technique to monitor the activity of an important class of enzymes. Using a molecular beacon annealed to a DNA or RNA oligonucleotide, the progression of a helicase along its substrate can be monitored in real time. Unlike conventional gel-based helicase assays, fluorescence-based assays—and in particular, the new molecular beacon–based helicase assay—are easily amenable to high-throughput screening. Moreover, these new assays differ from previously described continuous helicase assays (7–10,25,26) in three critical ways. First, all modifications are made on only one strand of the helicase substrate. Second, these assays monitor a decrease in fluorescence. Third, the products form hairpins, making the reaction essentially irreversible during the timescale of the experiment.

The fact that both the fluorophore and quencher are part of the same strand is important because it is increasingly recognized that helicases contact one strand of a duplex more than the other, displacing the complementary strand but making fewer specific contacts with it (13,14). In previously reported helicase assays, both strands are normally modified with a fluorophore on one strand and a quencher on the complement. As a result, the modification on either strand could influence helicase progression. To avoid this potential complication, both modifications are made on the strand believed to interact least with the helicase.

If this assay is to be used with a helicase other than the HCV helicase, appropriate substrates will need to be designed. The substrates used here were designed with a 3′ single-stranded tail sequence because the HCV helicase requires a 3′ single-stranded tail for optimal activity. Substrate requirements for other helicases vary widely. Other helicases likewise require 3′ single-stranded tails for optimal activity, whereas some require 5′ tails, some are bidirectional, some work at blunt ends or nicks, and some only act on forked substrates. It is also possible that some RNA helicases might not displace a DNA-based beacon from RNA. If that is the case, dual-labeled RNA probes could be used, but these are more difficult to synthesize and, at present, are expensive and not widely commercially available.

While many of the beacons used here were based on ones used in previous studies (29), the design of the HCV genome–based molecular beacon substrate was aided by the use of the publicly available software mFold (http://frontend.bioinfo.rpi.edu/applications/mfold). Commercial software is also available for designing molecular beacons, such as Beacon Designer (Premier Biosoft International, Palo Alto, CA, USA). Considering that molecular beacons are commonly used in quantitative PCR, it should be noted that molecular beacon–based helicase assays could be monitored using almost any commercially available real-time quantitative PCR apparatus.

The fact that the molecular beacon–based helicase assay monitors fluorescence decrease is notable because previous continuous helicase assays typically monitor the increase of fluorescence after a fluorophore-bearing strand is separated from a quencher-bearing strand. In such a setup where fluorescence increase is monitored, it is somewhat challenging to convert fluorescence change into a fraction of unwound substrate, especially if an end point is not immediately obvious. With these molecular beacon assays, typically >95% of the signal is lost when the beacon is displaced. As a result, data from a molecular beacon–based helicase assay can be easily converted to a percentage of duplex remaining, simply by calculating fractional fluorescence remaining (F/F_o) after subtracting background fluorescence. The resulting rates are almost identical to those obtained by conventional gel-based helicase assays but far more time points can be obtained per reaction, enabling a more rigorous kinetic analysis.

Probably the most important feature of a molecular beacon–based helicase assay is that it is essentially irreversible. To prevent substrates from re-annealing after strand separation, many assays add, at some point, a high concentration of a complementary ssDNA/ssRNA. Prior studies have reported diverse, and conflicting, impacts of these capture or trapping single-stranded oligonucleotides, ranging from greatly inhibiting the reaction (8) to actually increasing the observed reaction rate (34). A molecular beacon solves this problem, especially when it is annealed to a fully complementary strand that is also capable of forming a hairpin. As a result, initial rates observed in molecular beacon–based helicase assays are linear with both time and enzyme concentration.

In conclusion, molecular beacons enable the study of steady-state rates of helicase-catalyzed reactions in a true high-throughput manner. Such a tool should be valuable for mechanistic analyses, helicase inhibitor identification, and structure activity relationships.

ACKNOWLEDGMENTS

This work was supported by the National Institutes of Health (NIH; grant no. AI052395). We are grateful to Dr. Fred Jaffe and Gagandeep S. Narula for valuable technical support. This paper is subject to the NIH Public Access Policy.

COMPETING INTERESTS STATEMENT

The authors declare no competing interests.

REFERENCES

1. **Singleton, M.R., M.S. Dillingham, and D.B. Wigley.** 2007. Structure and mechanism of helicases and nucleic acid translocases. Annu. Rev. Biochem. *76*:23-50.
2. **Frick, D.N. and A.M. Lam.** 2006. Understanding helicases as a means of virus control. Curr. Pharm. Des. *12*:1315-1338.
3. **Matson, S.W., S. Tabor, and C.C. Richardson.** 1983. The gene 4 protein of bacteriophage T7. Characterization of helicase activity. J. Biol. Chem. *258*:14017-14024.
4. **Sivaraja, M., H. Giordano, and M.G. Peterson.** 1998. High-throughput screening assay for helicase enzymes. Anal. Biochem. *265*:22-27.
5. **Earnshaw, D.L. and A.J. Pope.** 2001. FlashPlate scintillation proximity assays for characterization and screening of DNA polymerase, primase, and helicase activities. J. Biomol. Screen. *6*:39-46.
6. **Zhang, L., G. Schwartz, M. O'Donnell, and R.K. Harrison.** 2001. Development of a novel helicase assay using electrochemiluminescence. Anal. Biochem. *293*:31-37.
7. **Raney, K.D., L.C. Sowers, D.P. Millar, and S.J. Benkovic.** 1994. A fluorescence-based assay for monitoring helicase activity. Proc. Natl. Acad. Sci. USA *91*:6644-6648.
8. **Houston, P. and T. Kodadek.** 1994. Spectrophotometric assay for enzyme-mediated unwinding of double-stranded DNA. Proc. Natl. Acad. Sci. USA *91*:5471-5474.
9. **Bjornson, K.P., M. Amaratunga, K.J. Moore, and T.M. Lohman.** 1994. Single-turnover kinetics of helicase-catalyzed DNA unwinding monitored continuously by fluorescence energy transfer. Biochemistry *33*:14306-14316.
10. **Earnshaw, D.L., K.J. Moore, C.J. Greenwood, H. Djaballah, A.J. Jurewicz, K.J. Murray, and A.J. Pope.** 1999. Time-resolved fluorescence energy transfer DNA helicase assays for high throughput screening. J. Biomol. Screen. *4*:239-248.
11. **Eggleston, A.K., N.A. Rahim, and S.C. Kowalczykowski.** 1996. A helicase assay based on the displacement of fluorescent, nucleic acid-binding ligands. Nucleic Acids Res. *24*:1179-1186.
12. **Tyagi, S. and F.R. Kramer.** 1996. Molecular beacons: probes that fluoresce upon hybridization. Nat. Biotechnol. *14*:303-308.
13. **Delagoutte, E. and P.H. von Hippel.** 2002. Helicase mechanisms and the coupling of helicases within macromolecular machines. Part I: Structures and properties of isolated helicases. Q. Rev. Biophys. *35*:431-478.
14. **Patel, S.S. and I. Donmez.** 2006. Mechanisms of helicases. J. Biol. Chem. *281*:18265-18268.
15. **Frick, D.N.** 2007. The hepatitis C virus NS3 protein: a model RNA helicase and potential drug target. Curr. Issues Mol. Biol. *9*:1-20.
16. **Kolykhalov, A.A., K. Mihalik, S.M. Feinstone, and C.M. Rice.** 2000. Hepatitis C virus-encoded enzymatic activities and conserved RNA elements in the 3′ nontranslated region are essential for virus replication in vivo. J. Virol. *74*:2046-2051.
17. **Lam, A.M. and D.N. Frick.** 2006. Hepatitis C virus subgenomic replicon requires an active NS3 RNA helicase. J. Virol. *80*:404-411.
18. **Borowski, P., J. Deinert, S. Schalinski, M. Bretner, K. Ginalski, T. Kulikowski, and D. Shugar.** 2003. Halogenated benzimidazoles and benzotriazoles as inhibitors of the NTPase/helicase activities of hepatitis C and related viruses. Eur. J. Biochem. *270*:1645-1653.
19. **Maga, G., S. Gemma, C. Fattorusso, G.A. Locatelli, S. Butini, M. Persico, G. Kukreja, M.P. Romano, et al.** 2005. Specific targeting of hepatitis C virus NS3 RNA helicase. Discovery of the potent and selective competitive nucleotide-mimicking inhibitor QU663. Biochemistry *44*:9637-9644.
20. **Boguszewska-Chachulska, A.M., M. Krawczyk, A. Najda, K. Kopanska, A. Stankiewicz-Drogon, W. Zagorski-Ostoja, and M. Bretner.** 2006. Searching for a new anti-HCV therapy: Synthesis and properties of tropolone derivatives. Biochem. Biophys. Res. Commun. *341*:641-647.
21. **Borowski, P., M. Lang, A. Haag, and A. Baier.** 2007. Tropolone and its derivatives as inhibitors of the helicase activity of hepatitis C virus nucleotide triphosphatase/helicase. Antivir. Chem. Chemother. *18*:103-109.
22. **Hsu, C.C., L.H. Hwang, Y.W. Huang, W.K. Chi, Y.D. Chu, and D.S. Chen.** 1998. An ELISA for RNA helicase activity: application as an assay of the NS3 helicase of hepatitis C virus. Biochem. Biophys. Res. Commun. *253*:594-599.
23. **Kyono, K., M. Miyashiro, and I. Taguchi.** 1998. Detection of hepatitis C virus helicase activity using the scintillation proximity assay system. Anal. Biochem. *257*:120-126.
24. **Hicham Alaoui-Ismaili, M., C. Gervais, S. Brunette, G. Gouin, M. Hamel, R.F. Rando, and J. Bedard.** 2000. A novel high throughput screening assay for HCV NS3 helicase activity. Antiviral Res. *46*:181-193.
25. **Porter, D.J., S.A. Short, M.H. Hanlon, F. Preugschat, J.E. Wilson, D.H.J. Willard, and T.G. Consler.** 1998. Product release is the major contributor to kcat for the hepatitis C virus helicase-catalyzed strand separation of short duplex DNA. J. Biol. Chem. *273*:18906-18914.
26. **Boguszewska-Chachulska, A.M., M. Krawczyk, A. Stankiewicz, A. Gozdek, A.L. Haenni, and L. Strokovskaya.** 2004. Direct fluorometric measurement of hepatitis C virus helicase activity. FEBS Lett. *567*:253-258.
27. **Lam, A.M., D. Keeney, P.Q. Eckert, and D.N. Frick.** 2003. Hepatitis C virus NS3 ATPases/helicases from different genotypes exhibit variations in enzymatic properties. J. Virol. *77*:3950-3961.
28. **Zhang, J.H., T.D. Chung, and K.R. Oldenburg.** 1999. A simple statistical parameter for use in evaluation and validation of high throughput screening assays. J. Biomol. Screen. *4*:67-73.
29. **Santangelo, P.J., B. Nix, A. Tsourkas, and G. Bao.** 2004. Dual FRET molecular beacons for mRNA detection in living cells. Nucleic Acids Res. *32*:e57.
30. **Gwack, Y., D.W. Kim, J.H. Han, and J. Choe.** 1997. DNA helicase activity of the hepatitis C virus nonstructural protein 3. Eur. J. Biochem. *250*:47-54.
31. **Levin, M.K., Y.H. Wang, and S.S. Patel.** 2004. The functional interaction of the hepatitis C virus helicase molecules is responsible for unwinding processivity. J. Biol. Chem. *279*:26005-26012.
32. **Wong, I., K.L. Chao, W. Bujalowski, and T.M. Lohman.** 1992. DNA-induced dimerization of the *Escherichia coli* rep helicase. Allosteric effects of single-stranded and duplex DNA. J. Biol. Chem. *267*:7596-7610.
33. **Gozdek, A., I. Zhukov, A. Polkowska, J. Poznanski, A. Stankiewicz-Drogon, J.M. Pawlowicz, W. Zagorski-Ostoja, P. Borowski, and A.M. Boguszewska-Chachulska.** 2008. NS3 peptide, a novel potent Hepatitis C virus NS3 helicase inhibitor, its mechanism of action and antiviral activity in the replicon system. Antimicrob. Agents Chemother. *52*:393-401.
34. **Beran, R.K., M.M. Bruno, H.A. Bowers, E. Jankowsky, and A.M. Pyle.** 2006. Robust translocation along a molecular monorail: the NS3 helicase from hepatitis C virus traverses unusually large disruptions in its track. J. Mol. Biol. *358*:974-982.

Received 21 December 2007; accepted 20 March 2008.

Address correspondence to David Frick, Department of Biochemistry and Molecular Biology, New York Medical College, Valhalla, NY 10595, USA. e-mail: david_frick@nymc.edu